Published by IOP Publishing for Sissa Medialab

Received: *December 11, 2023*
Accepted: *February 15, 2024*
Published: *May 10, 2024*

16th Topical Seminar on Innovative Particle and Radiation Detectors
Siena, Italy
25–29 September 2023

Validation of the diamond detectors for the Super Fragment Separator beam diagnostics

2024 JINST 19 C05009

M. Alfonsi,* C. Nociforo, M. Kiš, M. Träger, J. Galvis Tarquino, T. Blatz, C. Karagiannis, M. Winkler and H. Simon

GSI Helmholtzzentrum für Schwerionenforschung,
Planckstraße 1, 64291, Darmstadt, Germany

E-mail: m.alfonsi@gsi.de

Abstract: The Super-FRS at the FAIR accelerator complex will adopt Chemical Vapor Deposition diamond detectors as radiation-hard particle rate counters. Their role will be to monitor the beam transmission for beams with ions rates up to 10^7 ions/spill and to calibrate the other beam diagnostics devices that are in duty at higher beam intensities. The target vacuum chamber of the Super-FRS hosts a $7 \times 7\,\text{mm}^2$ single crystal diamond and a $25 \times 25\,\text{mm}^2$ polycrystalline diamond: they are required to detect crossing particles with high efficiency ($> 98\%$) in the case of heavy ion species (Ar to U), and to stand for several years in an environment in which they can potentially accumulate a dose of a few MGy per year. Laboratory measurements and beam test campaigns were arranged in the past years for the validation of the proposed sensors, in particular for the case of the polycrystalline technology. Here we report the outcome of the irradiation of a sensor based on a $20 \times 20\,\text{mm}^2$ polycrystalline diamond produced by Element Six, with high intensity 1 GeV/nucleon Pb and U beams at GSI (Darmstadt). The detector signal shape characteristics and the ion counting efficiency have been monitored by interleaving periods of low ions rates, to evaluate possible damages or performance degradation during and after a total bombardment of about 6×10^{11} heavy ions.

Keywords: Beam-line instrumentation (beam position and profile monitors, beam-intensity monitors, bunch length monitors); Diamond Detectors; Radiation-hard detectors; Solid state detectors

*Corresponding author.

https://doi.org/10.1088/1748-0221/19/05/C05009

Contents

1 Introduction

The Facility for Antiproton and Ion Research (FAIR) [1] close to completion in Darmstadt (Germany) will deliver relativistic ion beams, spanning from proton and light ions up to ^{238}U ions and with intensity up to 3×10^{11} ions/spill.

In the new in-flight magnetic separator, the Super Fragment Separator (Super-FRS) [2, 3], the high level of direct and indirect radiation at the production target demands that the target area [4] is specifically designed with durable, failure tolerant and extremely radiation-hard equipment, taking into account very limited access possibilities. This strongly limits the detector technologies of the beam diagnostics that can be employed. Furthermore, detectors front-end electronics can be located only on the outside of the iron shielding, which implies that the detector analog signals must be transmitted over 10–15 m before having an amplification stage. Figure 1 (left) shows the model of the target vacuum chamber.

The strategy for the primary beam intensity monitor is based on a combination of different particle detectors, each devoted to a specific intensity range, mounted on three drives (see figure 1, right picture) that can move the detectors in/out of the beam. The slot of each detector is chosen to allow for the mutual inter-calibration of two intensity monitor devices, in the common range of intensities in which both can operate.

The particle rate counters planned for primary beam intensities up to 10^7 ions/s are diamond detectors produced with a Chemical Vapor Deposition (CVD) process, namely a $7 \times 7\,\text{mm}^2$ single crystal diamond in the third ladder, the closest to the target position, and a larger $25 \times 25\,\text{mm}^2$ polycrystalline diamond in the first ladder crossed by the primary beam. They are expected to count uranium ions with a counting efficiency larger than 98% and a few % accuracy. At higher and at the highest intensities the primary beam particles count is obtained from the current drawn by, respectively, a Ionization Chamber (IC) and a Secondary Electron Transmission Monitor (SEETRAM) [5], after having calibrated this current with the counts rate from the diamond detectors.

The choice of diamond detectors as counting devices is motivated by their strong radiation hardness under different types of radiation as reported extensively in literature (e.g. [6–11]). Within the framework of the validation of diamond detectors for the Super-FRS, our group has already reported the radiation hardness of polycrystalline diamonds under high rate low energy 62 MeV/nucleon carbon

2024 JINST 19 C05009

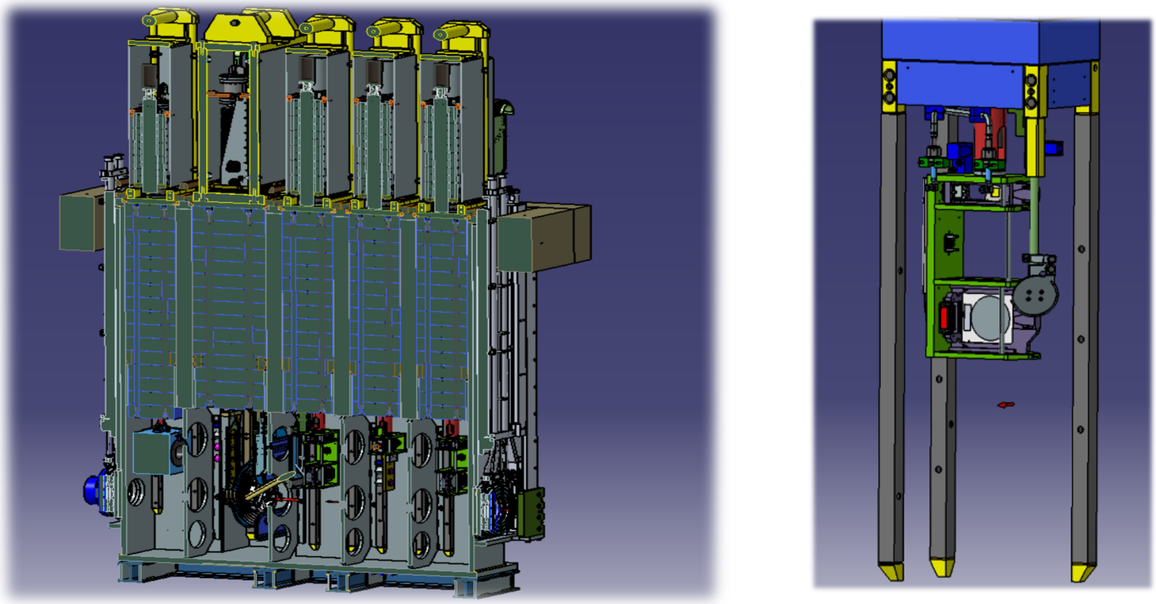

Figure 1. Model of the Super-FRS target chamber (left) and detail of the detectors ladder (right). The target vacuum chamber allows for the insertion of five 4 m tall "plugs", which include motion drives to move instrumentation in/out of the beam and the necessary radiation shield made out of iron. In the detail, the slots for the beam diagnostic devices of the first and third ladder from the right (the primary beam comes from the right of the picture) are visible. The target wheel is mounted on the fourth plug from the right. Courtesy of Michel Lindemulder, KVI-CART, University of Groningen, Netherlands.

ions exposure [12, 13]. In this article we report the results of two irradiation campaigns, performed in February and March 2021, of polycrystalline diamonds with 1025 MeV/nucleon ^{208}Pb beam and 1000 MeV/nucleon ^{238}U beam, respectively.

2 Experimental configuration and methods

A $20 \times 20\,\text{mm}^2$, 320 µm thick, polycrystalline diamond produced by Element Six (electrode size $18 \times 18\,\text{mm}^2$) was irradiated at the Fragment Separator (FRS) [14, 15] at GSI (Darmstadt).

The experimental setup was distributed among two focal planes of the FRS. In the diagnostic vacuum chamber of the first focal plane (S1) the polycrystalline diamond detector (PC) was installed inside an air pocket next to a ionization chamber (IC), see figure 2.

In the diagnostic vacuum chamber of the second focal plane (S2) a stack of four diamond detectors was installed on a motion drive. Two single crystal diamond detector ("SC3" and "SC6"), with a $3.2 \times 3.2\,\text{mm}^2$ and a 6 mm diameter active area and a 200 µm and 550 µm thickness, respectively, act as trigger devices and reference detectors in the data analysis. The other two samples are diamonds produced with a different process under study, although they were also used to further cross-checks.

The beam diagnostic devices available at the S1 and S2 focal planes were used at the beginning of the experiment to set up a beam optics that ensured the full transport of the ions from S1 to S2. Moreover, as additional counters independent from our setup, we recorded also the information from the SEETRAM in front of the FRS production target, whose current is proportional to the primary beam intensity, and the counts of the 5 mm thick, $220 \times 100\,\text{mm}^2$ large plastic scintillator at S2, located

2024 JINST 19 C05009

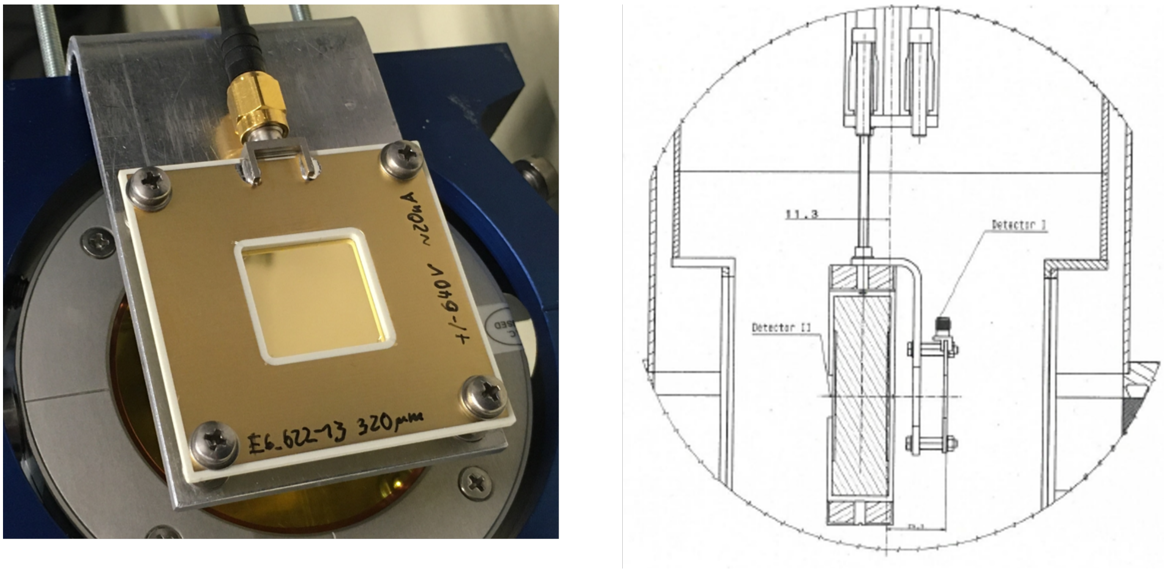

Figure 2. (Left) Picture of the crystalline diamond (PC) irradiated during the beam test campaigns, mounted in front of a ionization chamber. (Right) Technical drawing depicting the installation of the two detectors in the air pocket of the S1 focal plane.

just in front of the diamonds stack. We aimed at a beam size smaller than the PC active area at its location: along the horizontal axis this was ensured by the horizontal slits that are very close to the PC position, but no vertical slits are present in the S1 vacuum chamber and we cannot exclude that a small fraction of the beam was missing the PC while still hitting the plastic scintillator at S2.

The main goal was to study the effect of heavy ions intense irradiation on the counting efficiency of a polycrystalline diamond detector. For this reason, periods of high irradiation intensity have been interleaved with low particle rate periods, in which the performance of the PC has been measured in comparison to the reference diamond SC3. In contrast to the plastic scintillator, the smaller active area of the SC3 reference diamond ensured that any ion traversing it had also crossed the PC, so that the counting efficiency can be defined as the ratio of detection between the PC and the SC3. The second reference diamond SC6, slightly larger in active area, was used for cross-checks. To avoid deterioration of the performance of the reference devices during the high irradiation periods, not only the motion drives were used to take them out of the beam, but also the beam was dumped before reaching the S2 focal plane. On the contrary, the PC was never removed from the beam, although its bias voltage was reduced as low as 0.01 V/µm or, for the highest beam intensity, it was turned off.

The distance between the two focal planes was also the opportunity to experiment long signal transmission lines and signal amplification far from the signal source. A high quality 6 GHz bandwidth coaxial cable was adopted to transport, for about 50 m, the PC signal from the S1 focal plane to the S2 focal plane where the electronics and readout systems were installed. Here the PC signal was amplified with the broadband amplifier DBA3 [16]. No amplification was required for the two single crystal diamond reference devices.

We ran two independent acquisition systems in parallel. The (amplified) analog signals from the diamond detectors were split and sent to a 6 GHz bandwidth digital oscilloscope, where signal waveforms were acquired for offline analysis, as well as to discriminators and a standard VME-based

2024 JINST 19 C05009

system equipped with scalers and TDCs, controlled by the MBS acquisition system [17]. The currents drawn by the IC at S1 and the FRS SEETRAM were digitized with a current to frequency converter and the resulting pulses were counted with the VME scaler.

The trigger device of the MBS acquisition system was, depending on the dataset, either the plastic scintillator, or the single crystal diamond detector SC3, or the coincidence of the two. Nevertheless, in the data analysis we defined the counting efficiency always with respect to the coincidence of the plastic scintillator and the SC3 diamond. Since these devices exhibit sub-ns time resolutions, we further required a tight coincidence time window between the scintillator and SC3 signals, and in the PC counting efficiency computation only signals that occurred in a limited time window were taken into account to ensure that they were produced by the same crossing particle.

In addition, a 1 Hz clock was used as additional trigger in logical or, to have a constant sampling of the scaler counts even during the high intensity periods when all the devices that could act as trigger were taken out from the beam. The relative particle rate between all detectors obtained from the scaler counts, as well as their relative counting efficiency in defined time windows were monitored continuously, to make sure that undesired changes of the beam optics or unexpected loss of performance of the reference diamond detectors SC3 and SC6 did not occur.

3 Assessment of the accumulated ions

The number of accumulated ions in the two campaigns were assessed on the basis of the counts of all detectors on the VME scaler. The large plastic scintillator in S2 has been used as direct counter for all the low and middle intensity periods in which it was present in the beam. For the periods of high intensity in which the beam was dumped before the S2 focal plane, the current drawn by the IC has been used to assess the accumulated ions.

The relation between the frequency of the digitized pulses from the IC current and the counts of the plastic scintillator in S2 was studied in dedicated calibration datasets at low and middle beam intensity and cross-checked with all the periods with the plastic scintillator in the beam. The same approach was possible with the current drawn by the FRS SEETRAM in front of the production target, which provided a cross-check of the accumulated ions during the high irradiation periods and the only alternative for the peak intensities in which the IC digitized pulses rate reached a saturation. The linearity of the current digitizers employed for these two detectors was verified with a separate measurement before and after the beam time using an accurate low current generator. The SEETRAM digitizer allows to change the dynamic range to cover a wider span of currents, and all the available ranges were calibrated. The current offset of the two detectors generated a small rate of counts also without the passage of the beam. These quantities were monitored continuously in the inter-spill time, measured accurately during longer pauses of the beam delivery, e.g. beam area access, and subtracted in the definition of the detectors rates.

It is worth to highlight that this calibration between the IC or the SEETRAM current, and a counting device such as the plastic scintillator or the PC, represents also an exercise of the inter-calibration procedure during the Super-FRS operation.

The accumulation of ions in the two beam campaigns is presented in figure 3. Due to the different ions species employed, the two amounts are reported separately. The longer beam time of the first campaign in February 2021 allowed for three separate high intensity periods of several hours, accumulating about 6×10^{11} ions. This is comparable with the amount that is expected during one year of operation at the Super-FRS, including the full inter-calibration procedures that necessarily require a period at middle intensity to calibrate the target area IC and SEETRAM.

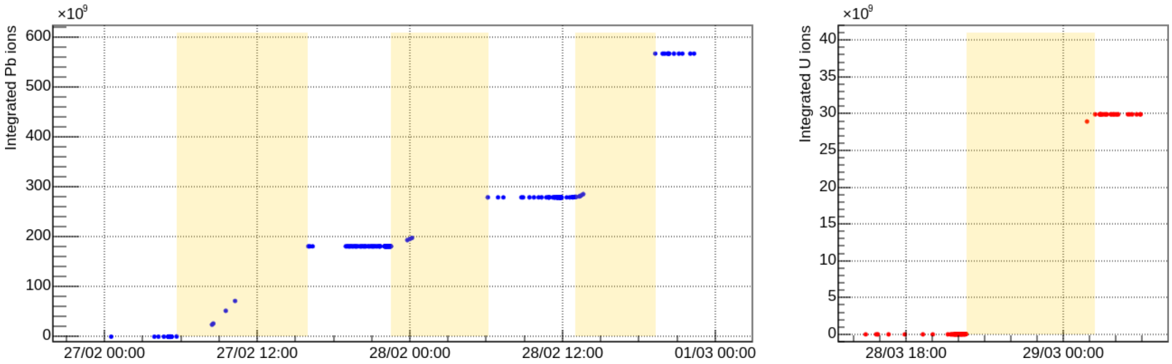

Figure 3. Accumulated ions during the two irradiation campaigns. Two ions species, namely lead and uranium, were used during the two campaigns, and the accumulation is reported separately in the left and right charts, respectively. The periods of high intensity beam are highlighted with yellow bands.

4 Irradiation effects on the counting efficiency

The PC counting efficiency was measured during each period of low intensity beam, for the bias voltage of 1 V/µm which is expected to be the reference setting at the beginning of the Super-FRS operation, as well as other voltages. The variation of this parameter is visible in figure 4.

The results of the February 2021 campaign show that the polycrystalline diamond is affected by radiation damage and the loss of performance becomes visible after the third irradiation period. After a bombardment of about 6×10^{11} lead ions, the counting efficiency drops to about 92% at a bias voltage setting of 1 V/µm. This setting is quite low if compared with the requirement for the Super-FRS diamond detector to be able to operate at 2 V/µm with a negligible leakage current. There is therefore enough room to continue to operate the same detector without replacement by increasing the bias voltage accordingly. This is demonstrated by the counting efficiency with the 1.5 V/µm bias voltage setting (red triangles in figure 4, left), which is still above the 98% requirement also at the end of the irradiation campaign in February.

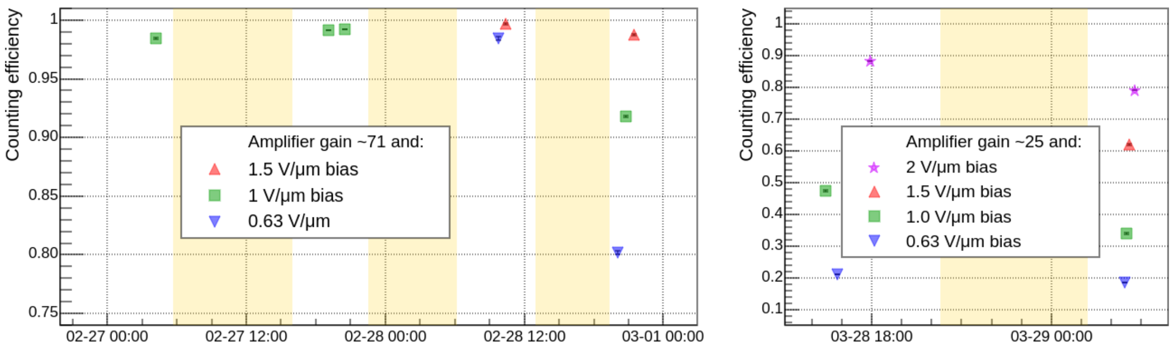

Figure 4. Variation of the counting efficiency of the polycrystalline diamond as it accumulated radiation, for the two campaigns and for different bias voltage setting. The values between two campaigns cannot be directly compared as two different gain setting of the amplifier were used.

The data of the March campaign are analyzed separately, since the amplifier gain used in March for the PC was smaller by a factor about 2.8 with respect the setting in February. This choice, which partly takes into account the higher ionization produced by the uranium projectile (about a factor 1.2 with respect to lead), was motivated by the optimization of the data acquisition of signals waveforms with the digital oscilloscope, to ensure the best exploitation of the oscilloscope dynamic ranges according to the voltage biases applied to the detector. The consequence for the counting efficiency analysis is that the presence of a performance degration due to radiation is very evident even at the highest bias voltage of 2 V/µm, since the signal amplitudes are always around the discriminators thresholds. On the other hand, these values are artificially lower and the results cannot be taken as representative of this detector technology. The study of the recorded signal waveforms can recover and even provide additional information on the effect of ions bombardment, if compared with the counting efficiency analysis, and results of this analysis will be published separately. The preliminary analysis finds a deterioration of the amplitude and the integrated charge of the signals after irradiation, which confirms that the loss in counting efficiency is real and not due to changes of the transport between focal planes or other external factors.

5 Conclusions

In February and March 2021 a large area CVD polycrystalline diamond produced by Element Six was irradiated with intense 1 GeV/nucleon lead and uranium beams at GSI. The goal was to validate the radiation hardness under heavy ions of the detector technology that has been proposed for one of the primary beam intensity monitor devices in the target area of the Super-FRS at the FAIR facility. The measurement setup built at the S1 and the S2 focal planes of the FRS allowed to evaluate the counting efficiency of this detector as it accumulates radiation, as well as to compute the total number of ions accumulated in the two campaigns. The latter represented also an exercise of the inter-calibration procedure between different intensity monitor devices that will be performed at the Super-FRS.

We observed a deterioration of the detector performance causing a drop of the counting efficiency at a bias voltage of 1 V/µm from above 98% to about 92% after being bombarded by about 6×10^{11} lead ions. This amount of radiation is comparable with one year of operation at the Super-FRS. On the other hand, the counting efficiency resulted still close to 99% and above the 98% Super-FRS specification at a bias voltage of 1.5 V/µm. The Super-FRS specifications require that the polycrystalline diamond detector can operate with negligible leakage current up to a bias voltage of at least 2 V/µm, hence providing a safe margin in which the bias voltage can be increased to recover the performance loss. In addition to the data for the counting efficiency evaluation, we recorded the signal pulse shapes with a digital oscilloscope. The variation of the signal shape parameters can provide further insight on the effects of the ion bombardment and the results will be published separately.

Finally, in this test we measured the heavy ion counting efficiency of a $5 \times 5\ \mathrm{mm}^2$, 303 µm thick, heteroepitaxial diamond grown on iridium, provided by the University of Augsburg, and mounted in the stack at S2 together with the reference single crystal diamonds. It demonstrated a counting efficiency fulfilling the 98% Super-FRS requirement also with an signal amplification of a factor ~ 25, therefore better performance than a polycrystalline diamonds. Large wafers can be produced with this technology, which therefore may represent an alternative to polycrystalline diamonds for the Super-FRS.

2024 JINST 19 C05009

Acknowledgments

The authors acknowledge the FRS team for their professional technical support. We acknowledge also the German BMBF, the Hessian Ministry of Higher Education, Research, Science and the Arts, the Rhineland-Palatinate MWG, Thuringian Ministry of Economics, Science and Digital Society for the funding support of FAIR construction.

References

[1] Facility for Antiproton and Ion Research in Europe GmbH, http://www.fair-center.eu/.

[2] H. Geissel et al., *The Super-FRS project at GSI*, *Nucl. Instrum. Meth. B* **204** (2003) 71.

[3] M. Winkler et al., *The status of the Super-FRS in-flight facility at FAIR*, *Nucl. Instrum. Meth. B* **266** (2008) 4183.

[4] L.M. Orona et al., *Super-FRS Target Area Remote Handling: Scenario and Development*, *Int. J. Adv. Robot. Syst.* **10** (2013) 386.

[5] B. Jurado, K.H. Schmidt and K.H. Behr, *Application of a secondary-electron transmission monitor for high precision intensity measurements of relativistic heavy-ion beams*, *Nucl. Instrum. Meth. A* **483** (2002) 603.

[6] T. Behnke, M. Doucet, N. Ghodbane and A. Imhof, *Radiation hardness and linearity studies of CVD diamonds*, *Nucl. Phys. B Proc. Suppl.* **125** (2003) 263 [hep-ex/0212018].

[7] HADES collaboration, *Radiation damage in single crystal CVD diamond material investigated with a high current relativistic* ^{197}*Au beam*, *Nucl. Instrum. Meth. A* **763** (2014) 1.

[8] C. Bauer et al., *Recent results from the RD42 Diamond Detector Collaboration*, *Nucl. Instrum. Meth. A* **383** (1996) 64.

[9] E. Alemanno et al., *Radiation damage of polycrystalline diamond exposed to 62 MeV protons*, *Nucl. Instrum. Meth. A* **730** (2013) 152.

[10] V. Grilj et al., *Irradiation of thin diamond detectors and radiation hardness tests using MeV protons*, *Nucl. Instrum. Meth. B* **306** (2013) 191.

[11] RD42 collaboration, *Radiation tolerance of diamond detectors*, *J. Phys. Conf. Ser.* **2374** (2022) 012172.

[12] S. Schlemme et al., *Long-term exposure of a polycrystalline diamond detector irradiated by 62 MeV/nucleon carbon beams*, *Diam. Relat. Mater.* **99** (2019) 107536.

[13] F. Schirru et al., *Evaluation of the counting efficiency of a pcCVD diamond detector irradiated by 62 MeV/nucl. carbon beams*, 2020 *JINST* **15** C04040.

[14] H. Geissel et al., *Ions penetrating through ion-optical systems and matter — non-liouvillian phase-space modelling*, *Nucl. Instrum. Meth. A* **282** (1989) 247.

[15] H. Geissel et al., *The GSI projectile fragment separator (FRS): A versatile magnetic system for relativistic heavy ions*, *Nucl. Instrum. Meth. B* **70** (1992) 286.

[16] P. Moritz et al., *Broadband electronics for CVD-diamond detectors*, *Diam. Relat. Mater.* **10** (2001) 1765.

[17] J. Adamczewski-Musch, N. Kurz and S. Linev, *Status and developments for DAQ system MBS v6.3*, GSI Scientific Report (2014) [DOI:10.15120/GR-2015-1-FG-CS-05].

2024 JINST 19 C05009